TSINGHUA SCIENCE AND TECHNOLOGY
ISSN 1007-0214 10/13 pp323–332
DOI: 10.26599 / TST.2018.9010038
Volume 23, Number 3, June 2018

# Efficient Helicopter−Satellite Communication Scheme Based on Check-Hybrid LDPC Coding

Ping Wang, Liuguo Yin*, and Jianhua Lu

**Abstract:** When implementing helicopter−satellite communications, periodical interruption of the received signal is a challenging problem because the communication antenna is intermittently blocked by the rotating blades of the helicopter. The helicopter−satellite channel model and the Forward Error Control (FEC) coding countermeasure are presented in this paper. On the basis of this model, Check-Hybrid (CH) Low-Density Parity-Check (LDPC) codes are designed to mitigate the periodical blockage over the helicopter−satellite channels. The CH-LDPC code is derived by replacing part of single parity-check code constraints in a Quasi-Cyclic LDPC (QC-LDPC) code by using more powerful linear block code constraints. In particular, a method of optimizing the CH-LDPC code ensemble by searching the best matching component code among a variety of linear block codes using extrinsic information transfer charts is proposed. Simulation results show that, the CH-LDPC coding scheme designed for the helicopter−satellite channels in this paper achieves more than 25% bandwidth efficiency improvement, compared with the FEC scheme that uses QC-LDPC codes.

**Key words:** helicopter−satellite communications; check-hybrid; Low-Density Parity-Check (LDPC) codes; Extrinsic Information Transfer (EXIT); iterative decoding

## 1 Introduction

Helicopter−satellite communications have attracted considerable attention in recent years due to their various applications, such as rescue missions after disasters, fire fighting, and aerial observation[1]. When an emergency occurs, helicopter−satellite communication is an especially interesting alternative because it allows faster deployment than terrestrial communication networks. However, the helicopter−satellite communication has been left out of other rapidly developing forms of mobile satellite communications because of propagation impairment, which is known as periodical blockage caused by the rotating blades of the helicopter[2].

Historically, conventional helicopter−satellite communication systems have to use a landline relay station to avoid rotor blades blockage[3], which limits the available area for helicopter activity within 60−70 km from the relay station. Communication of conventional systems becomes unstable because of the influence of mountains and tall buildings and even becomes impossible when roads are cut. Some earlier approaches have attempted to transmit burst signals during blockage-free periods based on synchronization with the blades[4]. However, pilot symbols and receiver synchronization make these approaches sensitive to the dynamics of platform

- Ping Wang is with Department of Electronic Engineering, Tsinghua University, Beijing 100084, China, and with the EDA Laboratory, Research Institute of Tsinghua University in Shenzhen, Shenzhen 518057, China. E-mail: p-wan14@mails.tsinghua.edu.cn.
- Liuguo Yin is with School of Information Science and Technology, Tsinghua University, Beijing 100084, China, and with the EDA Laboratory, Research Institute of Tsinghua University in Shenzhen, Shenzhen 518057, China. E-mail: yinlg@tsinghua.edu.cn.
- Jianhua Lu is with Department of Electronic Engineering, Tsinghua University, Beijing 100084, China. E-mail: lhh-dee@mail.tsinghua.edu.cn.

* To whom correspondence should be addressed.
Manuscript received: 2017-11-03; accepted: 2017-11-27

movement. Nowadays, direct helicopter−satellite communications without relay stations, which involves delivering immediate on-the-move communications, may benefit from the advanced Forward Error Control (FEC) coding in reconstituting the received signal[5, 6].

Recently, Low-Density Parity-Check (LDPC) codes over helicopter−satellite channels have received considerable interest due to their powerful performance and low decoding complexity. In Ref. [5], the LDPC concatenated Bose−Chaudhuri−Hocquenghem (BCH) codes of Digital Video Broadcasting−Satellite−Second Generation or DVB-S2[7], which feature a long block length of 16 200 bits and 64800 bits, were employed to mitigate the rotor blade blockage. In Ref. [6], a very low-rate LDPC coding scheme (rate-1/9 and rate-2/9) was used to deliver data transmission through intermittent blockages caused by rotary wings. Codes with shorter block length for fast re-acquisition at a lower rate in Ref. [6] achieve the same decoding performance as the rate-1/2 mode of DVB-S2, however inevitably at the expense of great bandwidth expansion.

One particularly attractive class of structured LDPC codes for practical applications is the Quasi-Cyclic LDPC (QC-LDPC) code[8–10]. However, QC-LDPC codes are not strong enough in helping correct erasure errors in helicopter−satellite channels, because most QC-LDPC codes are designed for Additive White Gaussian Noise (AWGN) channels. The work of Refs. [11, 12] replaces the Single Parity-Check (SPC) code constraints in an LDPC code by the first-order Reed−Muller (RM) code constraints and BCH code constraints, respectively, and also introduces the degree-1 nodes attached to the communication channel, which can be considered a special kind of Generalized LDPC (GLDPC) codes. Such SPC-constrained GLDPC code can better handle erasure errors, with much more powerful component codes involved. However, extra check bits of component codes transmitted over the communication channel yield severe rate loss, making SPC-constrained GLDPC codes impractical for data transmission over helicopter−satellite channels.

In this paper, a class of Check-Hybrid LDPC (CH-LDPC) codes is constructed for a periodically blocked channel. The CH-LDPC code is generalized from the QC-LDPC code, which can moderate the code rate loss of the GLDPC code with hybrid check code constraints: the SPC code constraints and the component code constraints. Then, Extrinsic Information Transfer (EXIT) charts are used to optimize the code ensembles, as long as EXIT functions of CH-LDPC codes over the periodic blockage are established in this paper instead of the time-consuming Monte Carlo method used in Refs. [11, 12]. In previous works, SPC-constrained GLDPC codes are optimized by searching the degree distribution of local LDPC codes[11, 12]. Our approach is different in that the local QC-LDPC code is fixed and we search the best matching component code from a variety of linear block codes, because many kinds of linear block codes satisfy the SPC constraint, such as first order RM codes, BCH codes, and simplex codes.

Taking bandwidth utilization and power consumption into account, we design a CH-LDPC code with code rate of 2/7 and block length of 427 bits over helicopter−satellite channels in this paper. Simulation results show that the proposed CH-LDPC codes show better capability to deal with blockage than the QC-LDPC codes, and the bandwidth efficiency of our transmission scheme based on the CH-LDPC codes improves by 28.6% compared with the QC-LDPC codes over the periodical blockage channels.

The remainder of the paper is organized as follows: Section 2 describes the channel model of helicopter−satellite communications. Next, Section 3 presents a brief introduction of QC-LDPC codes and the SPC-constrained GLDPC codes. Section 4 presents the CH-LDPC code construction. In particular, the CH-LDPC code ensembles are optimized using EXIT charts in this section. Then, Section 5 examines the performance of the proposed codes over the helicopter−satellite channel with iterative decoding. We conclude the paper in Section 6.

## 2 Channel Model

Given the installation restriction of helicopters, the communication antenna is usually mounted on the tail boom or the rear fuselage, which is just under the rotor blades. Once the helicopter is hovering or in flight, the rotor blades will periodically block the antenna, consequently resulting in periodical fading of the received signal. The received signal fading can be modeled as a rectangular window fading, as shown in Fig. 1. The maximum reduction $A_b$ from the mean signal level can reach 10 dB to 30 dB, which is far beyond the accommodate ability of the link budget.

The time when two blades sweep over the antenna one behind the other is called the blockage period $T_p$, which is inversely proportional to the product of the rotor angular speed $V_r$ and the number of the blades $N_b$, that is, $T_p = 1/(V_r \times N_b)$. For a given helicopter type, we can observe

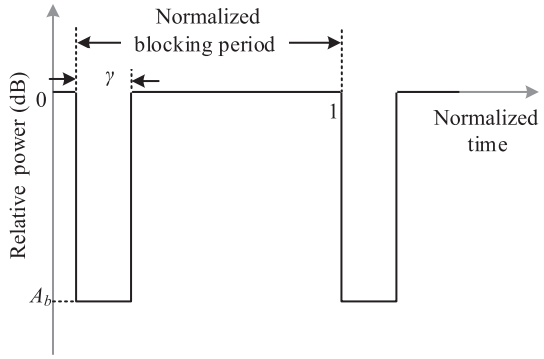


**Fig. 1 Power level fading of the helicopter−satellite signals.**

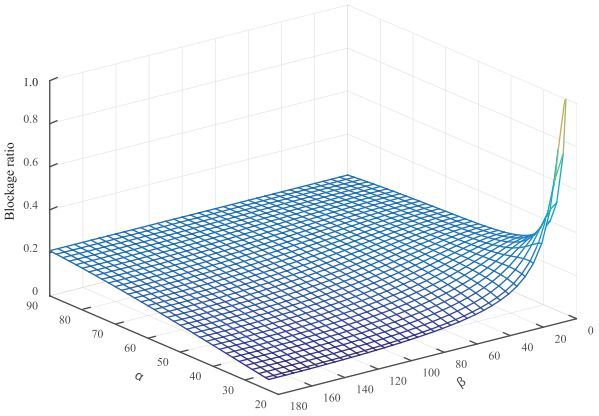


**Fig. 3 Blockage ratios of four pieces of blades.**

a constant blockage period which is independent of flight speed and heading direction, because the rotor angular speed remains constant.

However, the specific blockage duration period $T_d$ varies with the contribution from the elevation angel of the antenna and airframe orientation. The blockage duration period $T_d$ can be calculated as follows:

$$T_d = \frac{L_a + L_b \sin\alpha}{V_r \times 2\pi D} \tag{1}$$

where $L_a$ and $L_b$ represent the antenna aperture and the width of the blade, respectively. As shown in Fig. 2, $D$ is the equivalent distance that decides the severity of blockage. $D$ is decided by four parameters, namely, the horizontal distance from the hub to the antenna, $d$, the vertical distance from the blade to the antenna, $h$, the elevation angle of the antenna, $\alpha$, and the angle between the beam incident direction and the helicopter heading direction, $\beta$[13].

Therefore, the blockage ratio $\gamma = T_d/T_p$ varies for a given helicopter. Figure 3 shows the blockage ratios of a helicopter with four pieces of rotor blades under different elevation angles and orientation angles. As shown in Fig. 3, $\gamma$ varies from 0 to 1 and is mostly lower than 25%. Therefore, a qualified FEC scheme

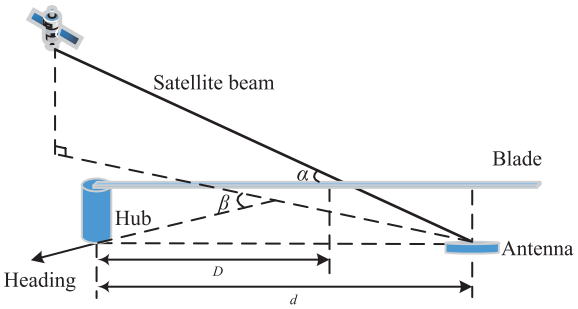


**Fig. 2 Side view of rotor blade blockage.**

for this helicopter−satellite system should at least enable communications under a 25% blockage. Helicopters with different pieces of blades will generally exhibit different blockage ratios. Table 1 shows blockage ratios for different pieces of blades. We can see that aircraft with smaller blade pieces generally exhibits lower blockage ratios than that with larger blade pieces.

Then, the received signal $r$ from helicopter−satellite channel can be calculated as Eq. (2).

$$r = h \cdot s + n \tag{2}$$

where $s$ is the transmitted signal, $h$ represents the blockage fading, and $n$ is the AWGN noise.

Traditionally, an interleaver is used to disperse burst errors over a long data sequence, allowing the helicopter−satellite channel with memory to be treated as a memoryless channel. We mainly focus on the coding performance. Specific interleaving methods are beyond the consideration of this paper. Thus, we consider that the transmitted data are evenly interleaved in this paper.

## 3 QC-LDPC Codes and SPC-Constrained GLDPC Codes

Following Ref. [8], we briefly introduce the definition of the QC-LDPC code. For the prime $p$, let $a$ and $b$, $a < b$, be

**Table 1 Blockage ratios for different numbers of blade pieces.**

| Number of blade pieces | Blockage ratio (%) |
|---|---|
| 2 | 12 |
| 3 | 18 |
| 4 | 25 |
| 5 | 30 |
| 6 | 38 |

divisors of $p-1$. Then, an $(a, b, p)$ regular QC-LDPC code can be represented by the following parity-check matrix $\boldsymbol{H}_{\mathrm{QC}}$.

$$\boldsymbol{H}_{\mathrm{QC}}=\begin{bmatrix} \boldsymbol{I}(p_{0,0}) & \boldsymbol{I}(p_{0,1}) & \cdots & \boldsymbol{I}(p_{0,b-1}) \\ \boldsymbol{I}(p_{1,0}) & \boldsymbol{I}(p_{1,1}) & \cdots & \boldsymbol{I}(p_{1,b-1}) \\ \vdots & \vdots & \ddots & \vdots \\ \boldsymbol{I}(p_{a-1,0}) & \boldsymbol{I}(p_{a-1,1}) & \cdots & \boldsymbol{I}(p_{a-1,b-1}) \end{bmatrix} \tag{3}$$

where $\boldsymbol{I}(p_{i,j})$, $i=0,1,\ldots,a-1$, $j=0,1,\ldots,b-1$, represents a $p\times p$ identity matrix with all rows cyclically shifted to the left by $p_{i,j}$ positions. The permutation number $p_{i,j}=\mathrm{mod}(q_1^i q_2^j, p)$, where $q_1$ and $q_2$ are two nonzero distinct elements of the Galois field GF($p$) with orders equal to $a$ and $b$, respectively.

In Ref. [8], the construction of irregular QC-LDPC codes is also proposed. For $0\leqslant i\leqslant a-3$, replacing the last $a-1-i$ circulant permutation matrices in the $i$-th row with zero matrices, the irregular QC-LDPC code with the same rate as the regular one is derived. Irregular QC-LDPC codes perform better than the corresponding regular QC-LDPC codes in waterfall region due to the smaller numbers of short cycles, because short cycles are known to deteriorate the decoding performance of LDPC codes. However, short cycles still exist in irregular QC-LDPC codes under most $a$ and $b$.

The SPC-constrained GLDPC code is introduced in Refs. [11, 12]. When constructing the SPC-constrained GLDPC code, the check node with degree $d_{\mathrm{c}}$ in the base LDPC code is generalized by a component code with information length equal to $d_{\mathrm{c}}-1$. First, each check node of the base LDPC code is replaced by a component code that satisfies the SPC constraint, and the generalized check nodes are called super check nodes. Then, the variable bits connected to each super check node are used to encode the component code. Extra check bits generated by component code encoding, except for the SPC-constrained bits, are transmitted over the channel together with the LDPC code. SPC-constrained GLDPC codes suffer an overall code rate loss, which is attributed to the higher error correcting capability of the component codes.

## 4 Check-Hybrid LDPC Coding Scheme

We illustrate the class of CH-LDPC codes in this section and adopt EXIT charts to optimize the CH-LDPC code ensembles. The CH-LDPC code is a generalization from the LDPC code and it has hybrid check code constraints: the SPC code constraints and more powerful component code constraints. The CH-LDPC code is actually a compromise between the LDPC code and the SPC-constrained GLDPC code, which is more suitable over helicopter−satellite channels. Specifically, on the one hand, the more powerful component code constraints in CH-LDPC code can better handle the fading and erasure errors in helicopter−satellite channels than the QC-LDPC code. On the other hand, unlike the GLDPC code, which results in severe code rate loss, the CH-LDPC code can accommodate its code rate more flexibly at different blockage ratios.

### 4.1 Code structure of the CH-LDPC code

The check matrix of an $(a,\ b,\ p)$ QC-LDPC has an $a$-layers structure, that is, $\boldsymbol{H}_{\mathrm{QC}}=[\boldsymbol{H}_0;\ \boldsymbol{H}_1;\ \ldots;\ \boldsymbol{H}_{a-1}]$. The proposed CH-LDPC code is a generalization from QC-LDPC code, where only one-layer SPC codes are replaced by the component codes. This concept is more easily understood in Fig. 4, which presents a different rendition of the Tanner graph. Figure 4 clarifies the notion that a CH-LDPC code has hybrid check node constraints, and the super check nodes in a CH-LDPC code generalized from the component codes also deliver bits transmitted over the communication channel as the variable nodes do. These extra bits are check bits generated by the component code encoding which we will introduce in the following encoding part. When considering which layer should be replaced, the middle layer is often the best choice, which can enable the component codes to join in as many small cycles in the base QC-LDPC code as possible.

By replacing one-layer check nodes of the $(a,\ b,\ p)$ QC-LDPC by the component code $C(n_{\mathrm{c}},k_{\mathrm{c}})$, we obtain a CH-LDPC code. If $p_{\mathrm{c}}$ bits of each component code are punctured, then the code rate will be calculated as Eq. (4).

$$R=\frac{b-a}{b+n_{\mathrm{c}}-k_{\mathrm{c}}-p_{\mathrm{c}}+1} \tag{4}$$

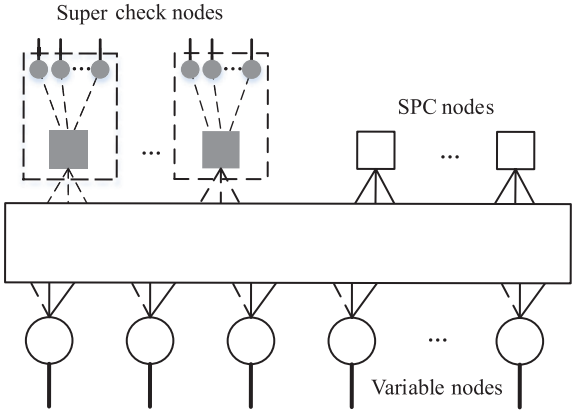


**Fig. 4 Graph representation of CH-LDPC codes.**

The CH-LDPC code introduces more powerful component codes than SPC codes, and moderates the code rate loss of GLDPC codes at the same time. For example, considering a (3, 6) regular QC-LDPC code, by replacing all the check nodes by (16, 5) first-order RM code, we can obtain a rate-0.083 GLDPC code. However, the CH-LDPC code replaces only one-layer check nodes, and a rate-0.1875 code is derived.

The component codes are required to satisfy the SPC constraint, that is, an all-ones column is needed in the systematic generator matrix of the component code. The first-order RM codes and BCH codes were adopted as the component codes in previous work[11, 12]. However, only half of the two kinds of codes satisfies the SPC constraint directly. The other half has to use nonsystematic generator matrices, which must execute data preprocessing before the component codes are encoded and decoded. Aside from the above two codes, the simplex codes are also adopted as component codes. The $(2^r-1, r)$ simplex code is always the dual code of the $(2^r-1, 2^r-r-1)$ Hamming code. Thus, the generator matrix of the simplex code is only the parity-check matrix of the Hamming code because of the dual code property for linear codes[14]. A systematic $(2^r-1, 2^r-r-1)$ Hamming code has a parity-check matrix $\boldsymbol{H}_{\text{Ham}}$ whose columns consist of all nonzero binary vectors of length $r$, which are each used once. Thus, we will always see an all-ones column in $\boldsymbol{H}_{\text{Ham}}$. Therefore, all simplex codes satisfy the SPC constraint, and no data preprocessing is needed.

### 4.2 Encoding and decoding of the CH-LDPC code

The CH-LDPC codeword can be derived from the base QC-LDPC code by the following two encoding steps:

(1) Base code encoding. We donate the generator matrix of a base QC-LDPC code as $\boldsymbol{G}_{\text{b}}$. Then, the code sequence of the QC-LDPC code can be given by $\boldsymbol{c}_{\text{b}} = \boldsymbol{u}\boldsymbol{G}_{\text{b}}$, where $\boldsymbol{u}$ is the information sequence.

(2) Component code encoding. The degree of freedom for an SPC-constrained check node with degree $k_{\text{c}}+1$ is $k_{\text{c}}$. Therefore, a component code with information length $k_{\text{c}}$ is needed when executing generalization. Given that $p$ check nodes with the same degrees are present in one-layer of the QC-LDPC code, let $\xi_i$, $i = 0, 1, \ldots, p-1$, represent the set of the first $k_{\text{c}}$ variable nodes connected to the $i$-th check node to be replaced. We denote $\boldsymbol{b}_i = [b_i(0),\ b_i(1),\ \ldots,\ b_i(k_{\text{c}}-1)]$ as the code bits in $\boldsymbol{c}_{\text{b}}$ that corresponds to $\xi_i$. We denote by $\boldsymbol{G}_{\text{c}} = [\boldsymbol{I}_{k_{\text{c}}} \quad \boldsymbol{Q}_{\text{c}}]$ the systematic generator matrix of the component code, and we denote $T$ as the column number of the all-ones column in $\boldsymbol{Q}_{\text{c}}$. Then, the check bits of component code are derived by $\boldsymbol{v}_i = \boldsymbol{b}_i\boldsymbol{Q}_{\text{c}}$. The $T$-th column of $\boldsymbol{Q}_{\text{c}}$ is an all-ones column. Thus, the $v_i(T)$ is exactly the SPC-constrained bit, and the SPC constraint can be interpreted as Eq. (5).

$$v_i(T) \oplus \sum_{j=0}^{k_{\text{c}}-1} b_i(j) = 0 \tag{5}$$

Taking $v_i(T)$ and the punctured bits out of $\boldsymbol{v}_i$, we obtain the rest of the check bits $\boldsymbol{v}_i^{'}$, which will be transmitted over the communication channel together with the base code sequence. Then, the CH-LDPC code sequence can be represented as the set $\boldsymbol{c} = [\boldsymbol{c}_{\text{b}},\ \boldsymbol{v}_0^{'},\ \boldsymbol{v}_1^{'},\ \ldots,\ \boldsymbol{v}_{p-1}^{'}]$.

The CH-LDPC code can be iteratively decoded by using the message passing algorithm based on the Tanner graph. During one iteration, all variable nodes and SPC-constrained check node decoders execute the same operations with the sum-product decoding algorithm of LDPC codes. For super check nodes, the trellis-based Maximum A Posteriori (MAP) decoding is typically used. Efficient low-complexity MAP decoding algorithms can be used to decrease the complexity of the decoder[15]. For the onboard decoder, the applications are constrained by the limited onboard resources and radiation protection requirements. We adopt the method in Ref. [16] to improve the reliability of memory in space radiation environments.

### 4.3 Code optimization based on EXIT charts

The iterative decoder structure of a CH-LDPC code is shown in Fig. 5. The Variable Node Decoder (VND) of a CH-LDPC code receives messages from both the communication channel and the extrinsic channel. The SPC-constrained Check Node Decoder (CND) receives messages from the extrinsic channel only. The super CND receives messages from both channels because the check

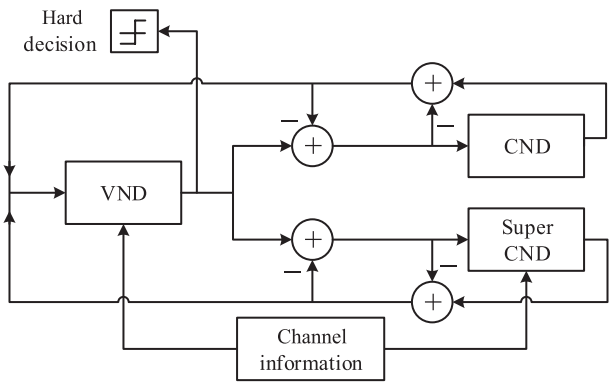


**Fig. 5 Iterative decoder for a CH-LDPC code.**

bits of the component codes are transmitted over the communication channel.

The helicopter−satellite channel can be treated as two instances of the AWGN channel with different signal-to-noise ratios $E_b/N_0|_0$ and $E_b/N_0|_1$, which correspond to the blockage free-period and blockage duration period respectively, where $E_b/N_0|_1 = E_b/N_0|_0 - A_b$ in decibel. From the aspect of constraint nodes, let $\alpha_j$, $j = 0,1$, represent the proportion of constraint nodes towards the AWGN instance with $E_b/N_0|_j$. Thus, we have $\alpha_0 = 1-\gamma$ and $\alpha_1 = \gamma$. Then, the EXIT functions of the CH-LDPC code over the periodical blockage channels can be calculated as

$$\begin{aligned} I_{\mathrm{E,V}} &= \Gamma_{\mathrm{V}}\left(I_{\mathrm{A,V}}, \left.\frac{E_b}{N_0}\right|_j\right) = \\ &\sum_i \lambda_i \sum_j \alpha_j I_{\mathrm{E,REP}}\left(I_{\mathrm{A,V}}, dv_i, \left.\frac{E_b}{N_0}\right|_j\right), \\ I_{\mathrm{E,C}} &= \Gamma_{\mathrm{C}}\left(I_{\mathrm{A,C}}, \left.\frac{E_b}{N_0}\right|_j\right) = \sum_i \rho_i I_{\mathrm{E,SPC}}(I_{\mathrm{A,C}}, dc_i) + \\ &\rho_{\mathrm{c}} \sum_j \alpha_j I_{\mathrm{E,Cmp}}\left(I_{\mathrm{A,C}}, \left.\frac{E_b}{N_0}\right|_j\right) \end{aligned} \tag{6}$$

where $\lambda_i$ represents the fraction of edges toward the variable nodes of degree $dv_i$, $\rho_i$ represents the fraction of edges toward the SPC-constrained check nodes of degree $dc_i$, and $\rho_{\mathrm{c}}$ represents the fraction of edges toward the super check nodes. $I_{\mathrm{E,REP}}(\cdot)$ and $I_{\mathrm{E,SPC}}(\cdot)$ represent the EXIT functions of the repetition code and the SPC code, which are the same as that in an LDPC code, and $I_{\mathrm{E,Cmp}}(\cdot)$ represents the EXIT function of the component code.

In Refs. [11, 12], the EXIT function of the super check node $I_{\mathrm{E,Cmp}}(\cdot)$ was obtained by using the Monte Carlo method. We derive the analytical expression function of $I_{\mathrm{E,Cmp}}(\cdot)$ below according to the split-encoders decoding model introduced in Ref. [17]. We first derive the EXIT function over the Binary Erasure Channel (BEC), and then convert it to the AWGN channel.

A decoding model with two split encoders is introduced in Ref. [17]. The encoder of a linear block code is split into two linear encoders. The encoded bits from encoder 1 are transmitted over a communication channel, while the encoded bits from encoder 2 are transmitted over an extrinsic channel. The EXIT function of a linear block code with split encoders under the MAP decoding is strongly connected to the split information functions. Moreover, the split information functions are decided by the split generator matrices. By applying the split-encoders decoding model to the super check node, we obtain the split generator matrices $\boldsymbol{G}_1 = \tilde{\boldsymbol{Q}}_{\mathrm{c}}$ and $\boldsymbol{G}_2 = [\boldsymbol{I}_{k_{\mathrm{c}}} \quad \boldsymbol{Q}_{\mathrm{c}}(T)]$ for encoders 1 and 2, respectively, where $\tilde{\boldsymbol{Q}}_{\mathrm{c}}$ represents the matrix $\boldsymbol{Q}_{\mathrm{c}}$ that excludes the all-ones column and the punctured columns, and $\boldsymbol{Q}_{\mathrm{c}}(T)$ is the all-ones column. The split information functions can then be calculated by support weights according to the split generator matrices. Although a considerable amount of computation is required when calculating the split information functions, this process is still feasible because we only adopt component codes with very short block lengths.

According to Ref. [17], the EXIT function of a linear block code over the BEC can be easily calculated after the split information functions are derived. If the block lengths of encoders 1 and 2 are $n$ and $m$, respectively, and if the erasure probabilities of the extrinsic and communication channels are $p$ and $q$, and the unnormalized split information function is $\tilde{e}_{i,j}, 0 \leqslant i \leqslant m, 0 \leqslant j \leqslant n$, then the EXIT function of a linear block code over the BEC can be represented as Eq. (7).

$$\begin{aligned} I_{\mathrm{E,Cmp}}^{\mathrm{BEC}} =& 1 - \frac{1}{m}\sum_{h=0}^{n}(1-q)^h q^{n-h} \sum_{g=1}^{m}(1-p)^{g-1} \cdot \\ & p^{m-g}[g\cdot\tilde{e}_{g,h} - (m-g+1)\cdot\tilde{e}_{g-1,h}] \end{aligned} \tag{7}$$

The component codes adopted in this paper are low-rate linear block code. Thus, the EXIT function over the AWGN channel can be derived from the EXIT function of its dual code over the BEC[18].

$$I_{\mathrm{E,Cmp}}^{\mathrm{AWGN}} \approx 1 - \frac{1}{\ln 2}\sum_{i=1}^{\infty}\frac{1}{2i(2i-1)} I_{\mathrm{E,Cmp}^{\perp}}^{\mathrm{BEC}}(\varepsilon_i, \eta_i) \tag{8}$$

where $\varepsilon_i$ and $\eta_i$ represent the erasure probabilities of the split channels, which can be converted from the mutual information over the AWGN channel.

In accordance with Eqs. (7) and (8) and dual property of EXIT functions in Eq. (9), analytical expression of the EXIT function for super check node can be derived.

$$I_{\mathrm{E,Cmp}^{\perp}}^{\mathrm{BEC}}(\varepsilon_i, \eta_i) = (1 - I_{\mathrm{E,Cmp}}^{\mathrm{BEC}}(1-\varepsilon_i, 1-\eta_i)) \tag{9}$$

In a CH-LDPC code, the split information functions of different eligible component codes are not univocal even under the same block length for encoders 1 and 2. We call this phenomenon the variety of split information functions, which is attributed to the dependence of the

split information functions on the specific representation chosen from generator matrices. For example, for a CH-LDPC code with a degree of super check node equal to 6, both (31, 5) simplex code and (15, 5) BCH code are eligible component codes. If four component check bits are transmitted over the communication channel, then the block lengths of encoders 1 and 2 are 6 and 4, respectively. Equations (10) and (11) give the corresponding unnormalized split information functions of simplex code and BCH code, which verifies the variety of split information functions.

$$\tilde{\boldsymbol{e}}_{7\times5\_\text{simplex}}=\begin{bmatrix}0&4&12&12&4\\6&48&107&93&28\\30&177&343&270&74\\60&306&534&384&100\\60&273&433&296&75\\30&120&180&120&30\\5&20&30&20&5\end{bmatrix} \tag{10}$$

$$\tilde{\boldsymbol{e}}_{7\times5\_\text{BCH}}=\begin{bmatrix}0&4&12&12&4\\6&48&108&94&28\\30&180&354&278&74\\60&312&552&392&100\\60&276&438&298&75\\30&120&180&120&30\\5&20&30&20&5\end{bmatrix} \tag{11}$$

Traditionally, SPC-constrained GLDPC codes are optimized by searching the degree distributions of base LDPC codes[11, 12]. Our approach is different in that the base QC-LDPC code is fixed and we search the best matching component code from a variety of linear block codes including the first-order RM codes, BCH codes, and simplex codes, according to the variety of split information functions.

In accordance with the convergence property of EXIT charts, we can form the optimization rules of CH-LDPC codes. Given a base QC-LDPC code, the CH-LDPC code ensemble can be optimized by minimizing the $E_b/N_0|_0$ concerning different component codes $C(n_\text{c},k_\text{c})$, on the premise that EXIT functions of VND and CND satisfy $\Gamma_\text{V}(\cdot)>\Gamma_\text{C}^{-1}(\cdot)$. Therefore, the optimization problem can be summarized as follows:

$$\begin{aligned}&\underset{C(n_\text{c},k_\text{c})}{\text{minimize}}\quad \left.\frac{E_b}{N_0}\right|_0,\\ &\text{s.t.}\quad \begin{cases}\Gamma_\text{V}(I_\text{A,V},\left.\frac{E_b}{N_0}\right|_0)>\Gamma_\text{C}^{-1}(I_\text{A,C},\left.\frac{E_b}{N_0}\right|_0),\\ \text{with}\quad k_\text{c}=dc-1.\end{cases}\end{aligned}$$

Two optimization results are derived, as shown in the following Examples 1 and 2 over the helicopter−satellite channel with 25% blockage, respectively. Short cycles in base QC-LDPC codes are eliminated by masking. Only the systematic component codes are considered in the optimization for easier encoding and decoding than the nonsystematic codes.

**Example 1**: The base code (girth=8) is masked from an irregular (723, 1928) QC-LDPC, with elements $p$=241, $a$=5, $b$=8, $q_1$=87, and $q_2$=8. The parity-check matrix is given by Eq. (12). The component codes are chosen from (16, 5) first-order RM code, (15, 5) BCH code, and (31, 5) simplex code. Each super check node transmits four check bits over the channel after encoding. Then, a rate-1/4 CH-LDPC code will be derived.

$$\boldsymbol{H}_\text{QC}=\begin{bmatrix}\boldsymbol{I}_1&\boldsymbol{I}_8&\boldsymbol{I}_{64}&\boldsymbol{I}_{30}&\boldsymbol{0}&\boldsymbol{0}&\boldsymbol{0}&\boldsymbol{0}\\\boldsymbol{I}_{87}&\boldsymbol{I}_{214}&\boldsymbol{I}_{25}&\boldsymbol{I}_{200}&\boldsymbol{I}_{154}&\boldsymbol{0}&\boldsymbol{0}&\boldsymbol{0}\\\boldsymbol{I}_{98}&\boldsymbol{I}_{61}&\boldsymbol{I}_{6}&\boldsymbol{I}_{48}&\boldsymbol{I}_{143}&\boldsymbol{I}_{180}&\boldsymbol{0}&\boldsymbol{0}\\\boldsymbol{I}_{91}&\boldsymbol{I}_{5}&\boldsymbol{0}&\boldsymbol{I}_{79}&\boldsymbol{I}_{150}&\boldsymbol{0}&\boldsymbol{I}_{201}&\boldsymbol{I}_{162}\\\boldsymbol{0}&\boldsymbol{0}&\boldsymbol{I}_{106}&\boldsymbol{I}_{125}&\boldsymbol{0}&\boldsymbol{I}_{47}&\boldsymbol{I}_{135}&\boldsymbol{I}_{116}\end{bmatrix} \tag{12}$$

By using the EXIT chart analyses, we obtain 1.507 dB as the decoding threshold of the rate-1/4 CH-LDPC code generalized from RM or BCH code and 1.651 dB as the decoding threshold of the rate-1/4 CH-LDPC code generalized from the simplex code over the helicopter−satellite channel with 25% blockage. EXIT charts of CH-LDPC codes employing different component codes at 1.507 dB and $\gamma$=25% are shown in Fig. 6. We can see that an iterative decoding tunnel exists for CH-LDPC code with BCH or RM code, while the tunnel of CH-LDPC code with simplex is closed. We therefore conclude that BCH or RM code is the best matching component code for

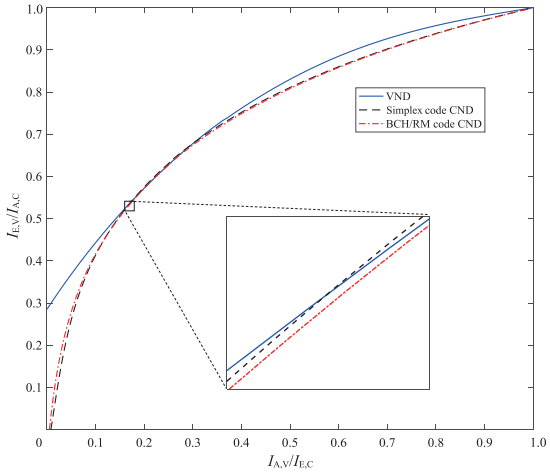


**Fig. 6 EXIT charts of rate-1/4 CH-LDPC code ensemble.**

the (723, 1928) base QC-LDPC code.

**Example 2**: The base code (girth=14) is masked from a regular (122, 305) QC-LDPC, with elements $p$=61, $a$=3, $b$=5, $q_1$=13, and $q_2$=9. The parity-check matrix is given by Eq. (13). The component codes are chosen from (15, 4) shortened first-order RM code, (14, 4) shortened BCH code, and (15, 4) simplex code. Each super check node transmits two check bits over the channel after encoding. Then, a rate-2/7 CH-LDPC code will be derived.

$$\boldsymbol{H}_{\mathrm{QC}}=\begin{bmatrix} \boldsymbol{I}_1 & \boldsymbol{I}_9 & \boldsymbol{I}_{20} & \boldsymbol{I}_{58} & \boldsymbol{0} \\ \boldsymbol{I}_{13} & \boldsymbol{I}_{56} & \boldsymbol{I}_{16} & \boldsymbol{I}_{22} & \boldsymbol{I}_{15} \\ \boldsymbol{I}_{47} & \boldsymbol{I}_{57} & \boldsymbol{I}_{25} & \boldsymbol{I}_{42} & \boldsymbol{I}_{12} \end{bmatrix} \tag{13}$$

By using the EXIT charts analyses, we obtain 2.101 dB as the decoding threshold of the rate-2/7 CH-LDPC code generalized from shortened RM or shortened BCH code and 1.995 dB as the decoding threshold of the rate-2/7 CH-LDPC code generalized from the simplex code over the helicopter−satellite channel with 25% blockage. EXIT charts of CH-LDPC codes that employ different component codes at 1.995 dB and $\gamma$=25% are shown in Fig. 7. From Fig. 7, we can see that different from the optimization result of Example 1, the simplex code is the best matching component code for the (122, 305) base QC-LDPC code.

## 5 Numerical Results

In this section, we demonstrate the decoding performance of the optimized CH-LDPC codes over the helicopter−satellite channels via binary phase-shift keying modulation. Considering a helicopter with four pieces of blades, the decoding performance of CH-LDPC codes under 10% blockage and 25% blockage is simulated. The maximum reduction $A_b$ is set to 30 dB.

Figure 8 shows the decoding performance of Example 1, i.e., a rate-1/4 CH-LDPC code with a block length of 2 892 bits over the helicopter−satellite channel. The decoding performance is compared with that of an LDPC code constructed by progressive edge growth[19] with the same rate and block length. Figure 8 shows that the designed CH-LDPC code outperforms the LDPC code by a fairly large margin at different blockage ratios.

Figure 9 shows the decoding performance of Example 2, i.e., a rate-2/7 CH-LDPC code with a block length of 427 bits, compared with the performance of a rate-2/9 QC-LDPC code with a block length of 900 bits, whose parameters are equivalent to the LDPC code adopted for periodical blockage channels in Ref. [6]. The performance of a rate-2/7 QC-LDPC code with a block length of 497 bits according to Ref. [8] is also illustrated for comparison. The designed CH-LDPC code shows better decoding performance than the rate-2/9 QC-LDPC code at different blockage ratios. From an engineering point of view, compared with the rate-2/9 coding scheme, bandwidth

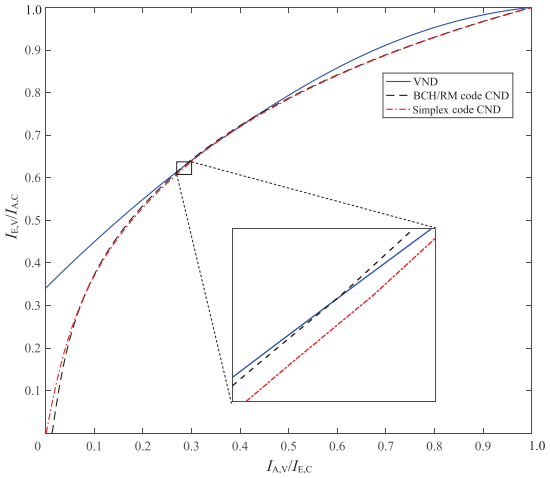


**Fig. 7 EXIT charts of rate-2/7 CH-LDPC code ensemble.**

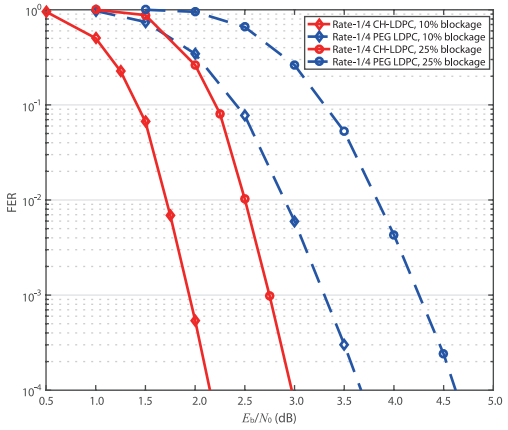


**Fig. 8 Decoding performance of rate-1/4 CH-LDPC code.**

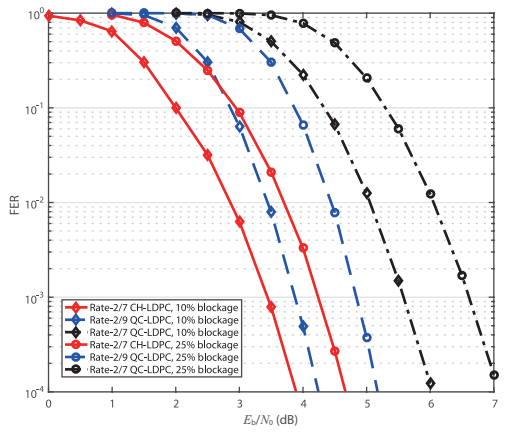


**Fig. 9 Decoding performance of rate-2/7 CH-LDPC code.**

efficiency improves by 28.6% with our rate-2/7 CH-LDPC coding scheme.

Despite its shorter block length, the proposed rate-2/7 CH-LDPC code shows better decoding performance than the rate-2/7 QC-LDPC code. Figure 10 shows the EXIT charts of these two codes under 10% blockage, respectively. When $E_b/N_0|_0 = 1.4$ dB, the VND curve and the CND curve of the QC-LDPC code intersect with one another, which indicates a decoding failure. However, a distinct iterative decoding tunnel still exists for the CH-LDPC code. Moreover, different from the fixed CND curve of an LDPC code, the CND curve of the CH-LDPC code moves down as $E_b/N_0|_0$ increases to 4 dB, which leads to a wider iterative decoding tunnel than the QC-LDPC code at the same $E_b/N_0|_0$ gap. This phenomenon in the EXIT charts of the CH-LDPC codes facilitates fast decoding convergence and benefits from the channel information involved during MAP decoding of the component codes. Moreover, we should note that, although it is not obvious from Fig. 10, the CND curve of the CH-LDPC code starts from a nonzero point due to the channel information involved.

## 6 Conclusion

Periodical signal fading caused by rotor blade blockage is one of the most severe impairments over helicopter−satellite channels. We study a class of CH-LDPC codes to mitigate such signal fading. The EXIT charts are presented as an engineering tool to optimize CH-LDPC code ensembles. Simulation results show that, our transmission scheme based on CH-LDPC coding achieves 28.6% higher bandwidth efficiency than the QC-LDPC codes over helicopter−satellite channels.

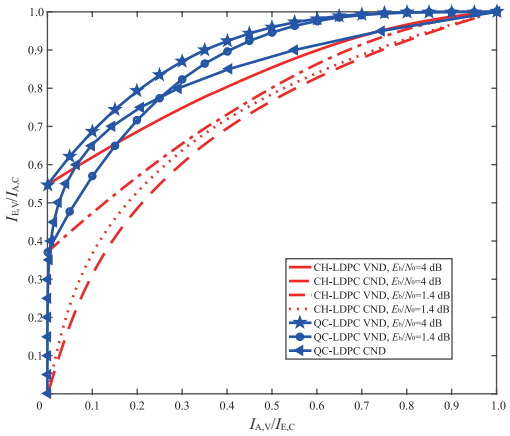


**Fig. 10 EXIT charts of rate-2/7 CH-LDPC code ensemble and rate-2/7 QC-LDPC code ensemble.**


### Acknowledgment

This work was supported by the National Natural Science Foundation of China (No. 91538203), and the new strategic industries development projects of Shenzhen City (No. JCYJ20150403155812833).


### References


[1] E. L. Cid, M. G. Snchez, A. V. Alejos, and S. G. Fernndez, Measurement, characterization, and modeling of the helicopter satellite communication radio channel, *IEEE Transactions on Antennas and Propagation*, vol. 62, no. 7, pp. 3776–3785, 2014.

[2] M. S. Reese, C. A. Balanis, C. R. Blncher, and G. C. Barber, Modeling and simulation of a helicopter-mounted satcom antenna array, *IEEE Antennas and Propagation Magazine*, vol. 53, no. 2, pp. 51–60, 2011.

[3] H. B. Li, M. Sato, A. Miura, S. Taira, and H. Wakana, Ku-band helicopter satellite communications for on scene disaster information transmission, in *IEEE International Symposium on Personal, Indoor and Mobile Radio Communications*, Barcelona, Spain, 2004, pp. 2792–2796.

[4] D. Wilcoxson, B. Sleight, J. O'Neill, and D. Chester, Helicopter ku-band satcom on-the-move, in *Proc. 2006 IEEE Military Communications Conference*, Washington, DC, USA, 2006, pp. 1–7.

[5] J. O'Neill, A. Loh, N. Velayudhan, and S. Har-Noy, Increased dynamic range multi-rate waveform for mobile satellite communications: Adaptive coding spreading and modulation (acsm), in *Proc. 2010 IEEE Military Communications Conference*, San Jose, CA, USA, 2010, pp. 357–362.

[6] L. N. Lee, V. Liau, W. Marhefka, and R. Gopal, Micro satellite terminal-based high data rate communication for rotary wing aircraft, in *Proc. 2014 IEEE Military Communications Conference*, Baltimore, MD, USA, 2014, pp. 1698–1703.

[7] M. Eroz, F. W. Sun, and L. N. Lee, An innovative low-density parity-check code design with near-shannon-limit performance and simple implementation, *IEEE Transactions on Communications*, vol. 54, no. 1, pp. 13–17, 2006.

[8] R. M. Tanner, D. Sridhara, A. Sridharan, T. E. Fuja, and D. J. Costello, Ldpc block and convolutional codes based on circulant matrices, *IEEE Transactions on Information Theory*, vol. 50, no. 12, pp. 2966–2984, 2004.

[9] H. Liu, Q. Huang, G. Deng, and J. Chen, Quasi-cyclic representation and vector representation of RS-LDPC codes, *IEEE Transactions on Communications*, vol. 63, no. 4, pp. 1033–1042, 2015.

[10] A. Yang, Z. Fei, C. Xing, M. Xiao, J. Yuan, and J. Kuang, Design of binary network codes for multiuser multiway relay networks, *IEEE Transactions on Vehicular*

*Technology*, vol. 62, no. 8, pp. 3786–3799, 2013.

[11] G. Yue, L. Ping, and X. Wang, Generalized low-density parity-check codes based on Hadamard constraints, *IEEE Transactions on Information Theory*, vol. 53, no. 3, pp. 1058–1079, 2007.

[12] Q. Li, X. Qu, L. Yin, and J. Lu, Generalized low-density parity-check coding scheme with partial-band jamming, *Tsinghua Science and Technology*, vol. 19, no. 2, pp. 203–210, 2014.

[13] X. G. Gou, J. H. Qiu, and H. J. Jiang, Research on antenna blockage from rotor in helicopter satellite communication, (in Chinese), *Radio Communications Technology*, vol. 39, no. 1, pp. 55–58, 2013.

[14] F. J. M. Williams and N. J. A. Sloane, *The Theory of Error-Correcting Codes*. New York, NY, USA: North-Holland Publishing Company, 1981, pp. 26–27.

[15] A. Ashikhmin and S. Litsyn, Simple MAP decoding of first-order Reed-muller and Hamming codes, *IEEE Transactions on Information Theory*, vol. 50, no. 8, pp. 1812–1818, 2004.

[16] G. Ge and L. Yin, LDPC coding scheme for improving the reliability of multi-level-cell nand flash memory in radiation environments, *China Communications*, vol. 14, no. 8, pp. 10–21, 2017.

[17] A. Ashikhmin, G. Kramer, and S. ten Brink, Extrinsic information transfer functions: Model and erasure channel properties, *IEEE Transactions on Information Theory*, vol. 50, no. 11, pp. 2657–2673, 2004.

[18] E. Sharon, A. Ashikhmin, and S. Litsyn, Exit functions for binary input memoryless symmetric channels, *IEEE Transactions on Communications*, vol. 54, no. 7, pp. 1207–1214, 2006.

[19] X. Y. Hu, E. Eleftheriou, and D. M. Arnold, Regular and irregular progressive edge-growth tanner graphs, *IEEE Transactions on Information Theory*, vol. 51, no. 1, pp. 386–398, 2005.

**Ping Wang** is currently working toward the PhD degree in the Department of Electronic Engineering, Tsinghua University, Beijing, China. She received the master degree from PLA University of Science and Technology, Nanjing, China in 2013. Her research interests include channel coding and satellite communications.

**Liuguo Yin** is a professor in the School of Information Science and Technology, Tsinghua University, Beijing, China. He received the MEng and PhD degrees from Tsinghua University, Beijing, China, in 2002 and 2005, respectively. From March 2005 to March 2007, he was a research assistant with the School of Aerospace, Tsinghua University. From April 2007 to March 2008, he was an ERCIM postdoctoral fellow with the Norwegian University of Science and Technology (NTNU), Trondheim, Norway. His research interests include channel coding, joint source-channel coding, wireless sensor networks, MIMO-OFDM systems, and wireless multimedia communication systems. He is a member of the IEEE Communications Society.

**Jianhua Lu** received the BEng and MEng degrees from Tsinghua University, Beijing, China, in 1986 and 1989, respectively, and the PhD degree in electrical and electronic engineering from the Hong Kong University of Science and Technology in 1998. Since 1989, he has been with the Department of Electronics Engineering, Tsinghua University, where he is currently a professor. He has published over 200 technical papers in international journals and conference proceedings. His current research interests include broadband wireless communications, multimedia signal processing, and satellite communications.

Prof. Lu is a fellow of the IEEE. He was a recipient of the best paper awards at the IEEE International Conference on Communications, the Circuits and Systems 2002, the ChinaCom 2006, and the IEEE Embedded-Com 2012. He served in numerous IEEE conferences as a member of Technical Program Committees. He was an editor of *IEEE Transactions on Wireless Communications* from 2008 to 2011, the Lead Chair of the General Symposium of the IEEE ICC 2008, and a Program Committee Co-Chair of the 9th IEEE International Conference on Cognitive Informatics in 2010, and a General Co-Chair at the 14th IEEE International Conference on Cognitive Informatics in 2015.

Prof. Lu is a member of the Chinese Academy of Sciences. He has made influential contributions to China's national major engineering programs, such as the Lunar Program. He was awarded the second prize of the National Technical Innovation Award and the second prize of the National Natural Science Award of China. He was granted the funding of the National Distinguished Young Scholar, and heading an Innovative Research Group of the National Natural Science Foundation of China. He was honored as the Yangtze River Scholar Distinguished Professor. He is currently a Chief Scientist of the National Basic Research Program (973) of China, and also serves as an Executive Member of the Council of the Chinese Institute of Electronics, and a Convener of the Discipline Appraisal Group of Information and Communication Engineering, Academic Degrees Committee of the State Council.